Suppression of the superconducting transition temperature of $CaSb_2$ by chemical substitution

Atsutoshi Ikeda[1,2]*, Shingo Yonezawa[2], and Yoshiteru Maeno[1]

[1]*Toyota Riken – Kyoto University Research Center, Kyoto University, Kyoto 606-8501, Japan*
[2]*Department of Electronic Science and Engineering, Kyoto University, Kyoto 615-8510, Japan*

We report on the crystal growth and superconducting transition temperature T_c of $CaSb_2$ with the chemical substitution for Ca. $CaSb_2$ is a line-nodal material with $T_c \simeq 1.7$ K. Although $CaSb_2$ exhibits the conventional superconductivity at ambient pressure, T_c shows an unusual peak under pressure. We found that T_c decreases with the substitutions of Sr and Ba for Ca, consistent with the effect of the negative chemical pressure.

$CaSb_2$ is a topological line-nodal material superconducting below T_c of about 1.7 K.[1)] Measurements of the nuclear quadrupole resonance revealed that its superconductivity is conventional at ambient pressure,[2)] and the temperature dependences of the specific heat and the penetration depth suggest fully gapped superconductivity with multiple Fermi surfaces.[3)] Curiously, T_c has a peak under hydrostatic pressure with the maximum of 3.4 K, which is twice larger than that at ambient pressure.[4)] Such a peak is unusual for the conventional superconductivity and cannot be explained by the change in the density of states.[5)] Theoretically, $CaSb_2$ is predicted to host Dirac nodal lines protected by the nonsymmorphic crystalline symmetry against the spin–orbit coupling in its electronic band structure.[6)] Quantum oscillations[7)] and the angle-resolved photoemission spectroscopy[8)] captured the band structure consistent with first-principles calculations. Moreover, a large magnetoresistance[6,7,9)] of 6,000% at 14 T and 1.8 K, attributable to the nodal lines, was observed.

In this paper, we report on the chemical substitution and evolution of T_c of $CaSb_2$. Our calculation suggests that one of the nodal lines comes closer to the Fermi energy E_F with the substitution of Sr for Ca, possibly enhancing the characters of Dirac nodal lines by band tuning to induce the theoretically predicted line-nodal superconductivity.[10)] Measurements of the AC susceptibility show that T_c decreases with Sr, Ba, and Eu. This result is consistent with the effects of the negative chemical pressure and of the magnetic impurity and indicates that one may be able to investigate the effects of physical pressure on the superconducting state via chemical pressure by suitable element substitution.

Single crystals of $Ca_{1-x}M_xSb_2$ (M = Sr, Ba, and Eu) were grown by the self-flux method using Sb as the flux. Ca (Sigma-Aldrich, 99.99%), Sr (Sigma-Aldrich, 99.99%), Ba (Furuuchi Chemical, 99.9%), and Eu (Rare Metallic, 99.9%) were melted in Sb (Rare Metallic, 99.9999%) with molar ratios of 1:4.0–1:4.7. We used alumina crucibles (Irie Corporation, SSA-S) for most of the samples, but for the Ba substitution we used a carbon crucible (Kyoto Takaoshin) to avoid the reaction between the crucible and Ba. For pure $CaSb_2$, the crucible was sealed in a quartz tube under 0.03 MPa of argon at room temperature and heated in a box furnace (Denken, KDF 80S) with a temperature profile similar to that reported in Ref. 7 but with the final temperature of 600°C instead of 610°C. For the substituted samples, the crucibles were sealed in quartz tubes under 0.07 MPa of argon at room temperature. The tubes were heated in a box furnace up to 780°C–800°C and then cooled down slowly to 580°C–600°C at a rate of −1°C/h. The remaining flux was removed by centrifugation. We obtained plate-shaped crystals with a few mm in diameter and less than 1 mm in thickness. We comment that attempt of Mg substitution resulted in chunk-shaped crystals, presumably $CaMg_2Sb_2$. Compositions of the samples were measured with the electron-probe microanalyzer (EPMA; JEOL, JXA-8105). The composition of the pure sample without substitution was measured to be Ca:Sb=34:66.

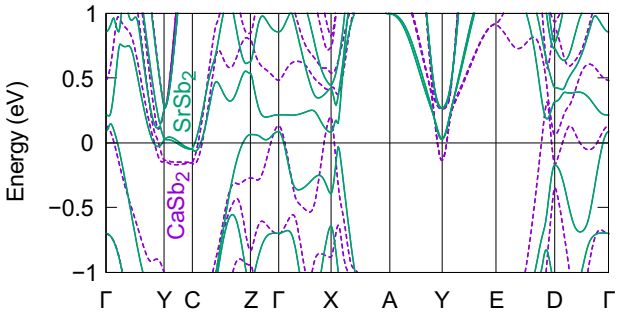

Fig. 1. (Color online) Calculated band structures of $CaSb_2$ (dashed curves) and $SrSb_2$ (solid curves). Positions of the high-symmetry points in the Brillouin zone are shown in Ref. 2.

AC magnetic susceptibility was measured with a lock-in amplifier (Stanford Research Systems, SR830) using a homemade susceptometer[11)] compatible with the adiabatic-demagnetization-refrigerator option of a commercial cryostat (Quantum Design, PPMS). We used a frequency of 19.997 kHz for the AC field. First-principles calculations were performed based on experimental crystal structures[12,13)] with the WIEN2k package[14,15)] using the Perdew–Burke–Ernzerhof generalized gradient approximation[16)] as the exchange–correlation functional.

We first present the calculated electronic band structures of $CaSb_2$ and $SrSb_2$ in Fig. 1. In $CaSb_2$, the bands forming the electron Fermi surfaces around the Y and C points host Dirac nodal lines. The flat bottom of the bands along the YC line is located 0.1–0.2 eV below E_F. As we substitute Sr for Ca and consequently apply negative chemical pressure, the band bottom is pushed up to E_F in $SrSb_2$ with the band bottom becoming more dispersive. Since we expect a larger contribution to the density of states at E_F from the bands forming nodal lines in $SrSb_2$ than in $CaSb_2$, we can study the interplay between nodal lines and superconductivity in $Ca_{1-x}Sr_xSb_2$.

Figure 2 shows the AC susceptibility of substituted crystals. Pure $CaSb_2$ exhibits a peak in the imaginary part at 1.68 K. Superconductivity is completely suppressed by a Eu substitution of 3%. This behavior is expected for the conventional superconductivity since Eu acts as a magnetic impurity. As we substitute Sr for Ca, T_c decreases systematically to 0.77 K at 8%. Substitution of Ba decreases T_c more significantly. These changes in T_c are attributable to the effect of the negative chem-

*ikeda.atsutoshi.3w@kyoto-u.ac.jp

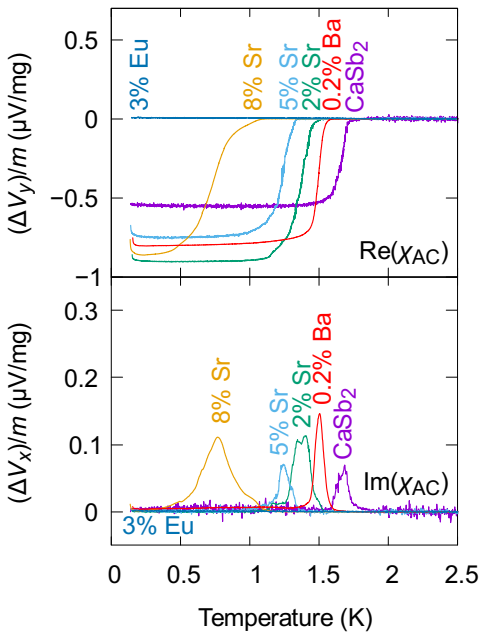

Fig. 2. (Color online) Temperature dependence of the AC susceptibility of $Ca_{1-x}M_xSb_2$ (M = Sr, Ba, and Eu). ΔV_x and ΔV_y represent the in-phase and out-of-phase components detected by the lock-in amplifier, respectively, parallel shifted so that the values become zero above 2 K. The signals are normalized by the mass m of each sample. The origin of the upturn in ΔV_y at the lowest temperature is unknown, possibly related to the instability of temperature or field.

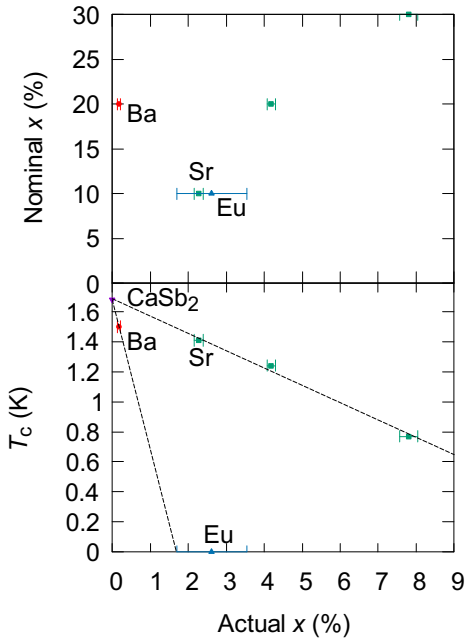

Fig. 3. (Color online) (top) Comparison between the nominal and actual amount of substitution in $Ca_{1-x}M_xSb_2$ (M = Sr, Ba, and Eu). The former is calculated from the molar ration of the starting reagents, and the latter was measured with the electron-probe microanalyzer. (bottom) Change in the superconducting transition temperature T_c with substitution of various elements.

ical pressure in contrast to the increase of T_c under hydrostatic pressure, since Ca has the smallest ionic radius among these three elements and Ba has the largest.

Figure 3 summarizes the relation between the actual and nominal amounts of substitution and T_c. For Sr and Eu, one-fifth to one-fourth of the starting reagents goes into the product, while for Ba only 0.7% is reflected in the sample. This difference should come from the different ionic radii. Linear extrapolation implies that T_c goes to 0 K at x = 15% for Sr and at x = 2% for Ba. Comparison of lattice parameters, density of states, and Debye temperatures of substituted samples would give a hint on the effect of different elements and on the unusual peak in T_c under physical pressure.

In summary, we succeeded in chemical substitution of Sr, Ba, and Eu for Ca in the single-crystalline superconducting nodal-line material $CaSb_2$. T_c decreases with Sr, Ba, and Eu substitutions; Ba has a stronger effect than Sr, and 3% of Eu substitution makes the superconductivity undetectable above 0.15 K. These features are attributable to the effect of the negative chemical pressure and the magnetic impurity. It would be an interesting future work to investigate if other superconducting properties change with Sr or Ba substitution as the bottom of the bands hosting Dirac nodal lines are lifted up to E_F. We hope this work triggers further material synthesis aiming at topological superconductivity in $CaSb_2$ and other Dirac materials.

Acknowledgment We acknowledge Tetsuo Kawakami and Fumiko Higashino for the measurements with EPMA. This work was supported by the Toyota Physical and Chemical Research Institute, North Campus Instrumental Analysis Station in Kyoto University, the Japan Society for the Promotion of Science (KAKENHI No. JP22H01168, No. JP22H04473, No. JP23H04861, and No. JP24K17011), ISHIZUE 2023 of Kyoto University, and the Murata Science Foundation. AI is supported by the Kyoto University Foundation.

References

1) A. Ikeda, M. Kawaguchi, S. Koibuchi, T. Hashimoto, T. Kawakami, S. Yonezawa, M. Sato, and Y. Maeno, Phys. Rev. Mater. **4**, 041801(R) (2020).
2) H. Takahashi, S. Kitagawa, K. Ishida, M. Kawaguchi, A. Ikeda, S. Yonezawa, and Y. Maeno, J. Phys. Soc. Jpn. **90**, 073702 (2021).
3) W. Duan, J. Zhang, R. Kumar, H. Su, Y. Zhou, Z. Nie, Y. Chen, M. Smidman, C. Cao, Y. Song, and H. Yuan, Phys. Rev. B **106**, 214521 (2022).
4) S. Kitagawa, K. Ishida, A. Ikeda, M. Kawaguchi, S. Yonezawa, and Y. Maeno, Phys. Rev. B **104**, L060504 (2021).
5) H. Takahashi, S. Kitagawa, K. Ishida, A. Ikeda, S. R. Saha, S. Yonezawa, J. Paglione, and Y. Maeno, Phys. Rev. B **109**, L100501 (2024).
6) K. Funada, A. Yamakage, N. Yamashina, and H. Kageyama, J. Phys. Soc. Jpn. **88**, 044711 (2019).
7) A. Ikeda, S. R. Saha, D. Graf, P. Saraf, D. S. Sokratov, Y. Hu, H. Takahashi, S. Yamane, A. Jayaraj, J. Sławińska, M. B. Nardelli, S. Yonezawa, Y. Maeno, and J. Paglione, Phys. Rev. B **106**, 075151 (2022).
8) C.-W. Chuang, S. Souma, A. Moriya, K. Nakayama, A. Ikeda, M. Kawaguchi, K. Obata, S. R. Saha, H. Takahashi, S. Kitagawa, K. Ishida, K. Tanaka, M. Kitamura, K. Horiba, H. Kumigashira, T. Takahashi, S. Yonezawa, J. Paglione, Y. Maeno, and T. Sato, Phys. Rev. Mater. **6**, 104203 (2022).
9) M. Oudah, J. Bannies, D. A. Bonn, and M. C. Aronson, Phys. Rev. B **105**, 184504 (2022).
10) S. Ono, H. C. Po, and K. Shiozaki, Phys. Rev. Res. **3**, 023086 (2021).
11) S. Yonezawa, T. Higuchi, Y. Sugimoto, C. Sow, and Y. Maeno, Rev. Sci. Instrum. **86**, 093903 (2015).
12) K. Deller and B. Eisenmann, Z. Anorg. Allg. Chem. **425**, 104 (1976).
13) K. Deller and B. Eisenmann, Z. Naturforsch. B **31**, 1146 (1976).
14) P. Blaha, K. Schwarz, G. K. H. Madsen, D. Kvasnicka, J. Luitz, R. Laskowski, F. Tran, and L. D. Marks, *WIEN2k, An Augmented Plane Wave + Local Orbitals Program for Calculating Crystal Properties*, edited by K. Schwarz (Technische Universität Wien, 2018).
15) P. Blaha, K. Schwarz, F. Tran, R. Laskowski, G. K. H. Madsen, and L. D. Marks, J. Chem. Phys. **152**, 074101 (2020).
16) J. P. Perdew, K. Burke, and M. Ernzerhof, Phys. Rev. Lett. **77**, 3865 (1996).